Numerical simulations on laser absorption enhancement in hybrid metallo-dielectric nanostructured targets for future nuclear astrophysics experiments

G. Pirruccio (iD), D. Rocco (iD), C. De Angelis, G. Sorbello (iD), D. Mascali (iD), G. Torrisi, M. Frassetto, L. Malferrari, F. Odorici (iD), C. Altana (iD), G. Lanzalone (iD), A. Muoio, S. Tudisco (iD), R. Benocci, G. Gorini, and L. Palladino

ARTICLES YOU MAY BE INTERESTED IN

Lattice resonances in dielectric metasurfaces
Journal of Applied Physics **125**, 213105 (2019); https://doi.org/10.1063/1.5094122

Surface wave photonic quasicrystal
Applied Physics Letters **116**, 151104 (2020); https://doi.org/10.1063/1.5139267

Active control of near-field radiative heat transfer through nonreciprocal graphene surface plasmons
Applied Physics Letters **116**, 151101 (2020); https://doi.org/10.1063/1.5145224

Numerical simulations on laser absorption enhancement in hybrid metallo-dielectric nanostructured targets for future nuclear astrophysics experiments

View Online   Export Citation   CrossMark

G. Pirruccio,[1,a] (ID) D. Rocco,[2,3] (ID) C. De Angelis,[2,3] G. Sorbello,[4,5] (ID) D. Mascali,[5] (ID) G. Torrisi,[5] M. Frassetto,[6] L. Malferrari,[6] F. Odorici,[6] (ID) C. Altana,[5] (ID) G. Lanzalone,[5,7] (ID) A. Muoio,[5] S. Tudisco,[5] (ID) R. Benocci,[8,9] G. Gorini,[9,10] and L. Palladino[11,12]

AFFILIATIONS

[1]Instituto de Física, Universidad Nacional Autónoma de México, Apartado Postal 20-364, México D.F. 01000, Mexico
[2]Dipartimento di Ingegneria dell'Informazione, Università degli Studi di Brescia, via Branze 38, Brescia 25123, Italy
[3]National Institute of Optics (INO), Via Branze 45, 25123 Brescia, Italy
[4]Dipartimento di Ingegneria Elettrica, Elettronica e Informatica (DIEEI), Università degli Studi di Catania, Viale Andrea Doria 6, 95125 Catania, Italy
[5]INFN Laboratori Nazionali del Sud (LNS), via S. Sofia 62, 95123 Catania, Italy
[6]INFN sezione di Bologna, Viale B. Pichat, 6/2, 40127 Bologna, Italy
[7]Università degli Studi di Enna "Kore", Via delle Olimpiadi, 94100 Enna, Italy
[8]Dip. di Scienze dell'Ambiente e della Terra, Univ. di Milano Bicocca, Piazza della Scienza 1, 20126 Milano, Italy
[9]INFN sezione di Milano Bicocca, Piazza della Scienza 3, 20126 Milano, Italy
[10]Dip. di Fisica, Univ. di Milano Bicocca, Piazza della Scienza 3, 20126 Milano, Italy
[11]Dip. to MESVA, Università degli Studi dell'Aquila, Piazza S. Tommasi 1, 67010 L'Aquila, Italy
[12]INFN gruppo collegato LNGS, V. G. Acitelli 22, 67100 Assergi L'Aquila, Italy

[a]Author to whom correspondence should be addressed: pirruccio@fisica.unam.mx

ABSTRACT

The linear electromagnetic interaction between innovative hybrid metallo-dielectric nanostructured targets and laser in visible and IR range is investigated through numerical simulations. The obtained results rely on the optimization of a target based on metallic nanowires (NWs) to enhance light absorption in the visible range of the electromagnetic spectrum. The NWs are grown within the ordered nanoholes of an alumina substrate, thus, forming a plasmonic lattice with triangular symmetry. The remaining volume of the nanoholes on top of the NWs is sealed with a transparent layer of aluminum oxide that is suitable to be chemically modified for containing about 25% of deuterium atoms. The study presented here is carried out within the framework of a scientific program named PLANETA (Plasmonic Laser Absorption on Nano-Engineered Targets) aiming at investigating new laser–matter interaction schemes in the ns domain and for nuclear fusion purposes, involving especially the D–D reaction.

I. INTRODUCTION

The study of nuclear reaction rates in plasmas is one of the most important issues in modern science, with interdisciplinary implications in astrophysics, cosmology, etc. One of the main points is the role of the electron screening as a booster for a number of fusion events in stellar nucleosynthesis.[1] The investigation of this physics in laboratory plasmas requires sufficiently high densities in

the electron clouds and ion temperatures lying in the range of few hundreds of eV, not far from those occurring in the stellar cores. Thermalization of the whole plasma is another crucial aspect, since nuclear fusion events must be correlated univocally with plasma density and temperature if one wants, for instance, to extrapolate astrophysical factors. These requirements suggest that ns-pulsed laser generated plasmas are suitable for nuclear astrophysics studies. At power intensities $\gg 10^2$ W/cm^2, laser-generated plasmas supersonically expand in vacuum with ion temperatures of several hundreds of eV and 10^{20}–10^{21} cm^{-3} densities.[2] Under these conditions, the classical Debye screening factor becomes comparable with the one of the solar core.[3] These plasmas, having self-thermalization times in the range of ps, are in LTE (Local Thermal Equilibrium) for most of the expansion time, being the latter in the same order of magnitude of the pulse duration. Densities and temperatures needed for the observation of any nuclear fusion event depend on the kind of target that is used for the laser irradiation. Normally, the highest efficiency is reached on metals, but fusion for astrophysics deals with elements such as deuterium and tritium and, recently, boron. One of the most interesting reactions is the D–D, which is also very important for energetic purposes. It is challenging to reach the above-mentioned densities and temperatures starting from targets made of deuterated polymers. The research about new targets, which are able to embed such nuclear fusion fuel is, therefore, of paramount importance. Optimal targets should also allow a higher amount of nuclear reactions per pulse, and, thus, increased light absorbance. Other groups have tried to use modified target surfaces in different ranges of laser pulse duration and power intensities. For example, in Ref. 4, authors investigated the target-normal-sheath-acceleration produced by a laser intensity of 10^{16} W/cm^2 by using thin polyethylene foils; they also studied ion yields and maximum energies vs target thickness and other possible solutions such as the use of carbon nanotubes embedded inside a polymer. Other nanostructures obtained from thin plastic foils have been used, again in order to enhance the mechanism of laser-driven proton beam acceleration.[5] In particular, a 100 TW laser beam has been absorbed with a drastically higher efficiency by a monolayer of polystyrene nanospheres, leading to a consequent increase in the maximum proton energy and beam charge. In Ref. 6, a kind of laser much closer to the ones we are interested in (both in terms of irradiance and pulse length), operating at 10^8 W/cm^2, was focused onto single-crystalline Fe and single-crystalline Fe with 2% of Si targets in order to compare the results. An evident increase in the average kinetic energy was observed for the targets embedding nanostructures with also a more focused ionic jet. Complex nanostructures have been widely investigated in the fs laser-pulse domain, as described in Ref. 7. All the mentioned works have used nanostructures with different textures with respect to the ones we have proposed here and completely different laser power and pulse lengths. Although several attempts with nanostructured targets have been done, anyway ns-lasers are typically focused on metallic, unstructured targets.

Typically, light absorption efficiency of the Nd-YAG laser in the IR region for typical metallic bulk materials, such as Al, Au, and Ag, lies between 1% and 5%. Moreover, unstructured Ag still exhibits low absorption in the visible range of the electromagnetic spectrum

due to the high onset of its interband transitions. When considering the fs-laser domains, nanostructured targets have been used to boost nuclear reaction rates and x-ray emission, taking advantage of their very large surface-to-volume ratio. While simulations of the plasma dynamics and propagation of charged particles within the nanostructure have been carried out to explain the enhanced rate,[8] little attention has been paid to the interplay between the optical properties of the materials comprising the target, their dimensions, and geometrical arrangement. Nanostructured materials may exhibit a complex geometry-dependent optical response. They can be designed to sustain surface optical resonances able to dramatically enhance light absorption, even in poor absorbers[9–11] and nanoporous materials.[12] Metallic nanostructures, in particular, can benefit from surface plasmon modes, collective oscillation of the electron density, which concentrate on the field intensity in sub-wavelength regions of the surface.[13] Depending on the shape, dimensions, and permittivity, individual metallic nanoparticles and NWs may sustain localized multipolar optical resonances resulting in a great enhancement of their absorption cross section. These localized resonances may couple via near-field interactions, giving rise to collective plasmon modes.[14–17]

Moreover, diffractive coupling of localized resonances in ordered arrays of nanoparticles and NWs further extends the tunability of the optical properties of the whole nanostructure.[18–20] A judicious choice of materials and geometrical parameters can even result in the total absorption of the incident light in a thickness of hundreds of nanometers,[21–23] thus providing huge advantages in terms of localization of electromagnetic energy over nanometer distances.[24,25] This increase in energy density can also, possibly, decrease the incident laser power required to generate the plasma.

To efficiently excite plasmonic resonances, a precise and non-trivial combination of material parameters and dimensions is required. Care must be taken in choosing the material constituting the NWs: it should be as robust as possible to absorb the highest amount of energy without being destroyed in the early stages of the laser irradiation, while its permittivity should allow supporting optical resonances. Depending on the wavelength region of interest, a variety of materials can be used. Typical choices are Ag and Al for the visible, while Au is preferred for the near-infrared. On the other hand, Co, Ni, and Fe are attractive possibilities, as indicated in a previous experiment on the ns-laser plasma production.[26]

Our results have to be seen as a proof-of-principle investigation of how a nanostructured target based on alumina-plus-nanowires textures can be engineered and manufactured in order to maximize electromagnetic absorption at those wavelengths typical of ns-lasers for solid material ablation. In particular, we will focus on textures that allow the inclusion of nuclear fuel, such as deuterium, that has to be inherently embedded into the target. We, hereby, describe targets made of vertically aligned Ag NWs, sustaining localized plasmon resonances. The proposed nanostructure has been tuned to exhibit high absorbance in the visible range, although the NIR range can also be covered by changing its geometrical parameters. The choice of the wavelengths at which we perform our simulations is based on the laser that is available for the future measurements, which is centered at 532 nm; it has a pulse width of 6 ns, and it provides an intensity of about 4×10^{12} W/cm^2. The proposed NWs are optimized to absorb

and concentrate the incoming electromagnetic energy on their surface, taking full advantage not only of their aspect ratio but also of their optical properties.

We point out that the main scope of this work is to theoretically demonstrate the possibility to strongly confine the optical energy within nanometric volumes localized on the target surface with a precise geometrical optimization that enhances the linear coupling between electromagnetic radiation (of varying wavelengths and wave vectors) and the nanowire plasmonic array. The high-power ns-pulsed laser interaction and the associated nonlinear dynamics and plasma generation are not discussed here.

II. RESULTS AND DISCUSSION

A typical NW array is shown in Fig. 1 after chemical dissolution of the alumina template. In this sample, NWs have 40 nm diameter and about 8 μm length. They are produced by using consolidated techniques[27–29] at the INFN laboratory in Bologna. Samples of 1 mm thick 99.5% pure aluminum plates are anodized in an electrolytic cell with a 0.3M oxalic acid solution at 15 °C under a DC voltage of 40 V. The resulting alumina pores have an average diameter of 40 nm and an inter-pore distance of about 100 nm. Different ranges of pore sizes (20–200 nm) and inter-pore distances (40–400 nm) can be obtained by changing the anodization conditions, in terms of acid solution and voltage.[27] For our laser-plasma experiment, Ag NWs have been grown inside the alumina nanochannels through AC electrodeposition (50 Hz, 6 Vpp) in a 0.011M $AgNO_3$ and 0.1M $MgSO_4$ solution. The growth of the Ag NWs starts from the bottom of the alumina nanopores, and their height is determined by the process duration. The obtained NW structure is polycrystalline.

For the simulations, we consider a plasmonic lattice consisting of vertically aligned, Ag NWs arranged in triangular symmetry. Figure 2(a) shows a top view of the proposed periodic structure, whereas Fig. 2(b) depicts a sketch of its unit cell. The metallic cylindrical NWs, with radius r, are grown on an Al substrate, and they are surrounded by an alumina, dielectric medium (800 nm height) with refractive index equal to 1.77. The height of the metallic pillar, h, is fixed to 400 nm and the cell period a is 250 nm.
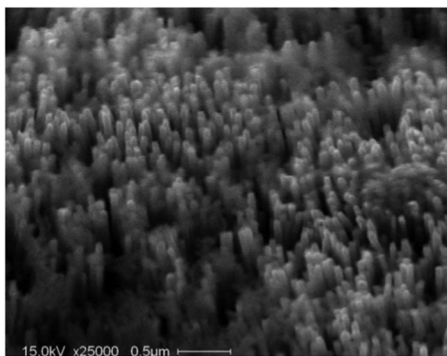

FIG. 1. Scanning electron microscopy image of the array of vertically aligned nanowires after alumina dissolution.
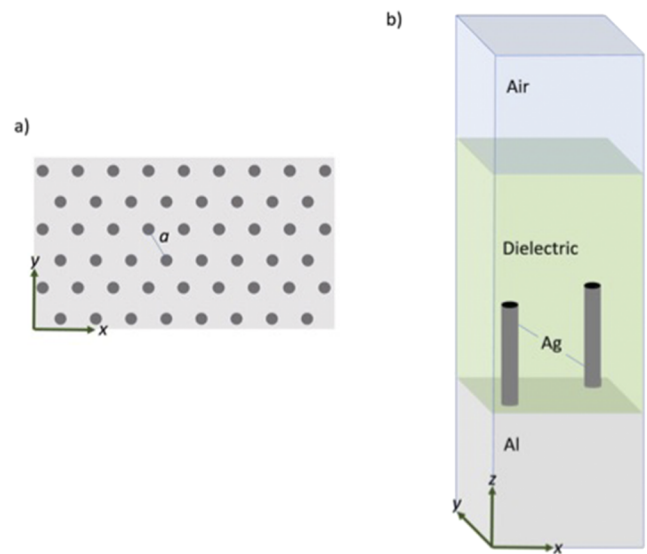

FIG. 2. (a) Plasmonic lattice with triangular symmetry (top view), a is the center-to-center NW distance. (b) Schematic sketch of the unit cell. The Ag cylindrical nanowires lie on an Al substrate and are embedded in an alumina dielectric environment. The top surface (black region) of the metallic pillar is where the nuclear reaction is supposed to take place.

For simulation purposes, the portion of the nanochannel above the nanowire (400 nm high) is also considered to be alumina, but technically it is possible to fill this region with an aluminum oxide containing up to 25% of deuterium atoms. Above the dielectric material, we considered an infinite layer of air. This type of arrays can support several types of optical modes: localized and diffractive. The former arises from the excitation of resonances in each metallic wire, while the latter comes from the long-range radiative coupling of all the wires and strongly depends on a. We will first look for the s-polarized localized modes, which for small radius and sufficiently large pitch are expected to show dipolar symmetry of the electric field. We perform finite element method (FEM) simulation using COMSOL Multiphysics. Since we are interested in the enhanced electric field intensity close to the top surface of the metallic nanowires (where the deuterium will be placed in the experiment), we assume a s-polarized plane wave excitation. We calculate the electromagnetic power dissipated by the Joule effect on the top surface of the Ag nanowires.

Figure 3(a) shows the electromagnetic power loss density, normalized to the incident power density, obtained for an incident angle between 0 rad and 0.6 rad by varying the pump wavelength in the case of nanowire radius equal to 20 nm. The incident wave provides momentum along the x axis, which corresponds to scanning the Γ–K high-symmetry trajectory of the first Brillouin zone. If other trajectories were to be considered, we may expect differences in the optical response of the nanostructure due to the different lattice parameters and scatterer density probed by the incident wave. The wavelength-incident angle plot represents the dispersion relation diagram of the optical modes sustained by the plasmonic lattice. An intense and non-dispersive feature, corresponding to the
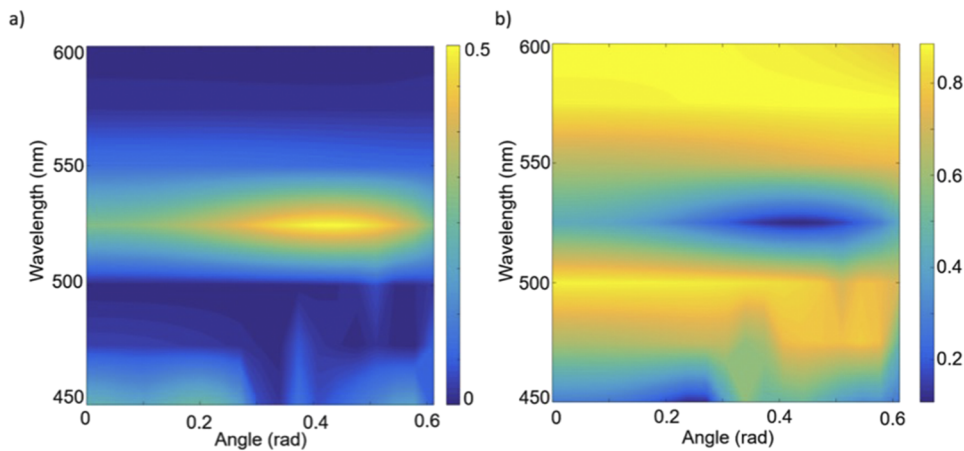
FIG. 3. (a) Calculated optical power density dissipated on the top surface of the Ag NWs normalized by the incident power. (b) Calculated reflectance as a function of the incident angle and wavelength. Both are calculated for a plasmonic lattice with a = 250 nm, h = 400 nm, and r = 20 nm.

maximum power dissipation, is obtained for a wavelength of 532 nm. We associate this resonance to the localized plasmon mode of the individual NWs. The value of the dissipated power shows a maximum for an incident angle of 0.43 rad. This can be explained by noting that the NWs do not possess a fully spherical symmetry; thus, a dependence of the power dissipation with the angle of incidence is expected. We also report the reflectance of the system $|S_{11}|$ in Fig. 3(b). Due to energy conservation, a minimum in the reflectance corresponds to a maximum of power dissipation. The transmittance is zero since the substrate is metallic. Very similar results are obtained in the case of the p-polarized incident plane wave (not shown here).

We have also verified that the addition of a 40 nm-thick dielectric layer below the NWs does not alter the results obtained (not shown here). The presence of this layer represents a more realistic sample because it is the "oxide barrier" that forms in a typical anodization process. We optimize the optical response of our nanostructure to the wavelength of one of our available lasers, i.e., 532 nm. Since we expect that the resonant wavelength is determined mostly by the NW radius, in Fig. 4, we simulate a plasmonic lattice with a cell period equal to 250 nm and h equal to 400 nm, illuminated by an s-polarized incident wave at an incident angle of 0.43 rad as a function of the NW radius. Figure 4 shows that the smaller the radius, the greater the power dissipation. We see that a radius of 20 nm of the Ag NWs can be considered optimum for our purpose. Moreover, this value is within the fabrication capabilities of our group.

In Fig. 5, we analyze the symmetry of the selected plasmonic mode. Figure 5(a) shows that the electric field intensity is dipolar, while Fig. 5(b) shows that the enhancement is localized at the top of each of the NWs. Nodes of the electric field intensity appear along the height of the NWs. These come from the interference of two counter-propagating plasmonic waves traveling to and reflected from the substrate, thus, forming a standing wave. We verified that the optical response of the lattice is not too sensitive to the chosen value of the height of the NWs. On resonance, a variation of 15% of the height leads only to a 10% variation of the dissipated optical power density. It should be noted that the electric field intensity enhancement reaches values of up to 400 in the

deuterium storage region. The concentration of optical energy in very small and localized regions may be useful to lower the laser incident intensity needed to create plasmas and reach astrophysical conditions. From the field confinement, we deduce that the NWs are optically weakly coupled, which provides a further justification to the dispersionless character of the mode (see Fig. 3). Other plasmonic modes that strongly couple the metallic nanowires may show an enhancement in other regions of the unit cell, i.e., above and in between the cylinders. We verify that by increasing the period up to 350 nm, the field enhancement of these coupled modes is, indeed, less local and more distributed in all the rest of the volume of the unit cell. These modes may be useful when the deuteron needs to be deposited not only on the top surface of the NWs but also on the rest of the alumina matrix. Since we are exploiting the plasmonic properties of the cylindrical nanowires, it is possible to
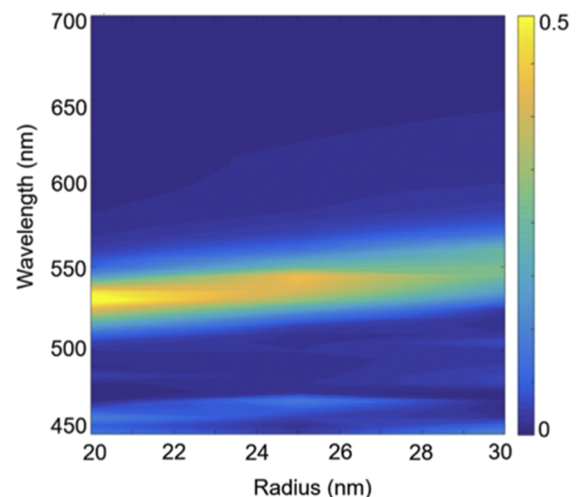

FIG. 4. Density power dissipation on the top surface of the Ag NWs for a plasmonic lattice with a = 250 nm and h = 400 nm, normalized to the incident power, as a function of the incident wavelength and NW radius r.

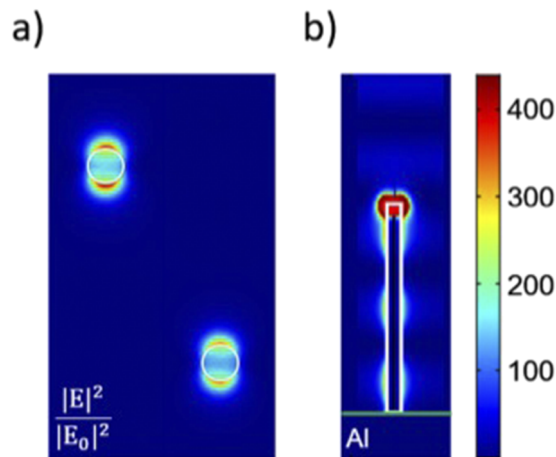**FIG. 5.** Electric field intensity enhancement for a plasmonic lattice with r = 20 nm, h = 400 nm, and a = 250 nm in the case of the s-polarized plane wave excitation with an incident angle of 0.43 rad; (a) top and (b) lateral views.

use heights comparable with the incident wavelength (hundreds of nanometers). Therefore, we argue that increasing the pillar height up to the micrometer scale, as shown in a previous work[8] is not necessarily needed to achieve full light absorption at the desired wavelength.

Importantly, we point out that our analysis is solely based on linear optical phenomena and disregards any thermodynamic effect. While it cannot be applied to describe the disruptive laser illumination, it can explain the response of the system before thermal dilatation (and subsequent evaporation) and free carrier absorption in the materials kick in.

III. CONCLUSIONS

We proposed a hybrid metallo-dielectric nanostructured target composed of ordered silver nanowires embedded in an alumina matrix, where the alumina pores (on top of the nanowires) can be filled-up with a deuterium-doped oxide. Our optimized design takes advantage of both geometry and optical properties of the materials to maximize light absorption in the region where deuterium is located. This study falls in the frame of a project aiming at studying the D–D fusion reaction rates, activated by high power laser irradiation. These reactions are expected to be boosted by the engineered enhanced local absorption and focusing properties of the nanowires. Our designed and numerically simulated target consists of a plasmonic lattice exhibiting a localized dipole plasmon resonance. In particular, we have shown that it is possible to find a structure in resonance with the specific wavelength of the incident laser that will be used in the future experiment. The optimal structure obtained by simulations is feasible for a real fabrication, upgrading the targets already fabricated at INFN-Bologna and preliminary tested at the LNS laser facility. This plasmonic mode is a good starting point to improve the optical performances of nanostructured targets for nuclear-astrophysics applications. The underlying hypotheses of the proposed study are the linear light–matter coupling and plasmonic

lattice regularity. We disregard any thermodynamic effect, including the target destruction dynamic, related to the laser pulse duration and the beam power density. The influence of the latter aspects needs to be experimentally verified. The present study is of potential interest, other than for fundamental studies in nuclear astrophysics, also for fusion science and technology.

DATA AVAILABILITY

The data that support the findings of this study are available from the corresponding author upon reasonable request.

REFERENCES

[1] E. Rolfs and W. S. Rodney, *Cauldrons in Cosmos* (University of Chicago Press, 1988).

[2] L. Torrisi, D. Mascali, R. Miracoli, S. Gammino, N. Gambino, L. Giuffrida, and D. Margarone, "Measurements of electron energy distribution in tantalum laser-generated plasma," J. Appl. Phys. **107**, 123303 (2010).

[3] E. E. Salpeter, "Electrons screening and thermonuclear reactions," Aust. J. Phys. **7**, 373 (1954).

[4] L. Torrisi, M. Cutroneo, and J. Ullschmied, "TNSA and ponderomotive plasma production in enriched carbon polyethylene foils," Phys. Plasmas **24**, 043112 (2017).

[5] D. Margarone, O. Klimo, I. J. Kim, J. Prokupek, J. Limpouch, T. M. Jeong, T. Mocek, J. Psikal, H. T. Kim, J. Proska, K. H. Nam, L. Stolcova, I. W. Choi, S. K. Lee, J. H. Sung, T. J. Yu, and G. Korn, "Laser-driven proton acceleration enhancement by nanostructured foils," Phys. Rev. Lett. **109**, 234801 (2012).

[6] A. Loruso, J. Krása, L. Láska, V. Nassisi, and L. Velardi, "Fe and Fe+2%Si targets as ion sources via UV laser ablation plasma," Eur. Phys. J. D **54**, 473 (2009).

[7] A. Lubcke, A. A. Andreev, S. Hohm, R. Grunwald, L. Ehrentraut, and M. Schnuren, "Prospects of target nanostructuring for laser proton acceleration," Sci. Rep. **7**, 44030 (2017).

[8] M. A. Purvis *et al.*, "Relativistic plasma nanophotonics for ultrahigh energy density physics," Nat. Photonics **7**, 796 (2013).

[9] S. Butun, S. Tongay, and K. Aydin, "Enhanced light emission from large-area monolayer MoS$_2$ using plasmonic nanodisc arrays," Nano Lett. **15**, 2700–2704 (2015).

[10] G. Pirruccio, M. Ramezani, and J. Gómez Rivas, "Enhancing light absorption in graphene with plasmonic lattices," Europhys. Lett. **119**, 17006 (2017).

[11] S. Butun, E. Palacios, J. D. Cain, Z. Liu, V. P. Dravid, and K. Aydin, "Quantifying plasmon-enhanced light absorption in monolayer WS$_2$ films," ACS Appl. Mater. Interfaces **9**, 15044–15051 (2017).

[12] R. Fazeli, "Letter efficient absorption of laser light by nano-porous materials with well-controlled structure," Laser Phys. Lett. **17**, 046001 (2020).

[13] S. Maier, *Plasmonics: Fundamentals and Applications* (Springer, 2007).

[14] D. Becerril, H. Batiz, G. Pirruccio, and C. Noguez, "Efficient coupling to plasmonic multipole resonances by using a multipolar incident field," ACS Photonics **5**(4), 1404–1411 (2018).

[15] E. Prodan, C. Radloff, N. J. Halas, and P. Nordlander, "A hybridization model for the plasmon response of complex nanostructures," Science **302**(5644), 419–422 (2013).

[16]M. Hentschel, M. Saliba, R. Vogelgesang, H. Giessen, A. P. Alivisatos, and N. Liu, "Transition from isolated to collective modes in plasmonic oligomers," Nano Lett. **10**(7), 2721–2726 (2010).

[17]M. Frimmer, T. Coenen, and A. F. Koenderink, "Signature of a fano resonance in a plasmonic metamolecule's local density of optical states," Phys. Rev. Lett. **108**(7), 077404 (2012).

[18]G. Weick et al., "Dirac-like plasmons in honeycomb lattices of metallic nanoparticles," Phys. Rev. Lett. **110**, 106801 (2013).

[19]V. G. Kravets, A. V. Kabashin, W. L. Barnes, and A. N. Grigorenko, "Plasmonic surface lattice resonances: A review of properties and applications," Chem. Rev. **118**(12), 5912–5951 (2018).

[20]W. Wang, M. Ramezani, A. I. Väkeväinen, P. Törmä, J. G. Rivas, and T. W. Odom, "The rich photonic world of plasmonic nanoparticle arrays," Mater. Today **21**, 303–314 (2018).

[21]T. V. Teperik, V. V. Popov, and F. J. Garcia de Abajo, "Total light absorption in plasmonic nanostructures," J. Opt. A: Pure Appl. Opt. **9**, S458 (2007).

[22]N. I. Landy, S. Sajuyigbe, J. J. Mock, D. R. Smith, and W. J. Padilla, "Perfect metamaterial absorber," Phys. Rev. Lett. **100**, 207402 (2008).

[23]H. Noh et al., "Perfect coupling of light to surface plasmons by coherent absorption," Phys. Rev. Lett. **108**, 186805 (2012).

[24]G. Pirruccio et al., "Coherent control of the optical absorption in a plasmonic lattice coupled to a luminescent layer," Phys. Rev. Lett. **116**, 103002 (2016).

[25]M. Ramezani, G. Lozano, M. A. Verschuuren, and J. Gomez-Rivas, "Modified emission of extended light emitting layers by selective coupling to collective lattice resonances," Phys. Rev. B **94**, 125406 (2016).

[26]A. Muoio, C. Altana, M. Frassetto, G. Lanzalone, L. Malferrari, D. Mascali, F. Odorici, and S. Tudisco, "Nanostructured targets irradiation by ns-laser for nuclear astrophysics applications: First results," J. Instrum. **12**, C03076 (2017).

[27]O. Jessensky, F. Müller, and U. Gösele, "Self-organized formation of hexagonal pore arrays in anodic alumina," Appl. Phys. Lett. **72**, 1173 (1998).

[28]R. Angelucci, F. Corticelli, M. Cuffiani, G. M. Dallavalle, L. Malferrari, A. Montanari, F. Odorici, R. Rizzoli, and G. P. Veronese, "A novel position detector based on nanotechnologies: The NanoChanT project," Nucl. Phys. B, Proc. Suppl. **125**, 164 (2003).

[29]L. Malferrari, A. Jagminiene, G. P. Veronese, F. Odorici, M. Cuffiani, and A. Jagminas, "Alumina template-dependant growth of cobalt nanowire arrays," J. Nanotechnol. **2009**, 149691.